

RSC Advances



This is an *Accepted Manuscript*, which has been through the Royal Society of Chemistry peer review process and has been accepted for publication.

Accepted Manuscripts are published online shortly after acceptance, before technical editing, formatting and proof reading. Using this free service, authors can make their results available to the community, in citable form, before we publish the edited article. This *Accepted Manuscript* will be replaced by the edited, formatted and paginated article as soon as this is available.

You can find more information about *Accepted Manuscripts* in the [Information for Authors](#).

Please note that technical editing may introduce minor changes to the text and/or graphics, which may alter content. The journal's standard [Terms & Conditions](#) and the [Ethical guidelines](#) still apply. In no event shall the Royal Society of Chemistry be held responsible for any errors or omissions in this *Accepted Manuscript* or any consequences arising from the use of any information it contains.



Poly(2-aminothiazole) as a unique precursor for nitrogen and sulfur co-doped porous carbon: Immobilization of very small gold nanoparticles and its catalytic application

Received 00th January 20xx,
Accepted 00th January 20xx

DOI: 10.1039/x0xx00000x

www.rsc.org/

Yasamin Bide, Mohammad Reza Nabid* and Fateme Dastar^a

In this contribution, we report two important achievements; first the synthesis of poly(2-aminothiazole) (P2AT) with a plate structure containing nanoparticles by a rapid initiated strategy, and second, the one-step synthesis of nitrogen and sulfur co-doped porous carbon materials with unique morphology using P2AT as the source of both N and S, through a simple hydrothermal carbonization reaction. The obtained functional carbon may serve to develop new carbon materials for various applications especially catalysis, because of the excellent properties, such as straightforward synthesis, defined morphology, high porosity, and heteroatom doping. As one of the most important applications, we used the porous carbon materials as a support for immobilizing gold nanoparticles (AuNPs). Benefiting from the synergistic effects of N and S co-doping, very small AuNPs, and unique structural features, the as-obtained material was demonstrated to be a superior catalyst for reduction of nitrobenzenes.

1. Introduction

The extensive availability of carbon-based materials and also their various physicochemical properties such as electrical conductivity, chemical and thermal stability as well as ability to approve different morphologies, make them suitable for wide applications such as energy storage,^{1, 2} catalysis,³⁻⁵ sorption, and chromatography. The high surface area and porosity are desirable properties for most of these applications and especially for catalysis.^{6, 7}

So, much efforts have been paid by the researchers to design new types of functional carbons through special precursors, surface decoration and meso-/nanopore engineering due to the their properties.⁸ The modification of carbon-based compounds through heteroatom doping may become the "Next Big Thing" in materials science.⁹ Because of the large electronegativity of nitrogen (3.04) in comparison with C (2.55),¹⁰ it is the most extensively adopted element among all doping elements. Improving the electric conductivity and increasing chemical stability are just two advantages of nitrogen doping.^{11, 12} Multiple doping as a useful synthetic approach for novel carbon materials modifies the carbon properties one step further compared to one-type-only heteroatom. The co-doping of nitrogen and the other elements such as P, B (with lower electronegativity than C), and S (similar electronegativity with C)^{13, 14} has been

investigated. Among them, sulfur doping in carbon materials is still quite rare and further research is expected due to its unique properties.¹⁵ According to the density functional theory (DFT) calculations conducted by Qiao et al, a synergistic interaction of the N- and S-dopants was existed probably because of an easier polarizability.¹⁶ Several methods such as in situ doping and post-treatment have been suggested to introduce heteroatoms into the carbon matrix.^{17, 18} Besides the more complicated process, the main disadvantage of post treatment strategy is the inhomogeneous distribution of heteroatoms and consequently ineffective improvement of the bulk properties. In contrast, the in situ doping method includes the direct carbonization of heteroatom-containing compounds such as ionic liquids or polymers which allows to obtain a homogeneous distribution of heteroatoms into the carbon matrix.¹⁹⁻²²

2-Aminothiazole (2-AT) as a nitrogen and sulfur-containing aromatic heterocyclic compound is a biologically active material with several useful properties such as anti-corrosion,²³ antimicrobial,²⁴ and antitumor.²⁵ So far, only a few reports exist on the polymerization of 2-AT,^{26, 27} which represents an emerging field in polymers research due to special structure of this polymer for modern applications. To the best of our knowledge, there is no report on employing rapid mixing reaction route for synthesis of P2AT that sufficient mixing can be easily attained by stirring or shaking before the polymerization begins.²⁸⁻³⁰ In this work, P2AT with a special plate structure containing nanoparticles was synthesized using rapid mixing polymerization, and then it was chosen as a single source precursor for synthesis of N and S co-doped porous carbon materials ((N, S)-PCM) through a hydrothermal carbonization route. Structurally, a mesoporous

^aFaculty of Chemistry, Department of Polymer, Shahid Beheshti University, G.C., P.O. Box 1983969411 Tehran, Iran. E-mail: m-nabid@sbu.ac.ir; Fax: +98 21 22431661; Tel: +98 21 29903102.

Electronic Supplementary Information (ESI) available. See DOI: 10.1039/x0xx00000x

and macroporous structure in the (N, S)-PCM is achieved. Chemically, the (N, S)-PCM displays a high number of heteroatom-doping, with N:C and S:C ratios of up to 1:4 and 1:13 (sulfur and nitrogen contents up to 4.45 and 14.2 at.%), respectively. We expected that, due to the high affinity of gold to S and N, the dual doped carbon support can enhance Au loading with uniform dispersion. Thanks to gold-based catalysts, numerous organic reactions have been reachable under simple conditions with both high yields and chemoselectivity.³¹ It should be notable that the catalytic activity of gold nanoparticles reduces considerably as the particle size grows beyond 10 nm.³²

As our continuing interest in the development of various nano-catalysts for organic transformations,^{21,22,33-37} herein, we employed gold nanoparticles immobilized on N and S co-doped porous carbon structure (AuNPs@(N, S)-PCM) for catalytic reduction of nitrobenzenes. The presence of hydrogen gas as a highly flammable substance can pose safety concerns.³⁸ So, the as prepared catalyst was employed for reduction of nitrobenzenes with NaBH₄ as the hydrogen source because of its non-flammability, easily hydrolyzable nature and controlled H₂ production rate.³⁹

This (N, S)-PCM not only presents a very promising material for catalytic applications, but also it can be employed in other fields such as lithium–air batteries, extraction, sensors, and drug delivery.

2. Experimental

2.1. Materials

Tetrachloroauric(III) acid trihydrate 99.5%, sodium hypochlorite solution, sodium borohydride, and 2-aminothiazole were purchased from Merck Chem. Co. All other chemicals were purchased from Aldrich or Merck companies and used as received without any further purification.

2.2. Instruments and characterization

Fourier transform infrared (FT-IR) spectra were recorded on a Bomem MB-Series FT-IR spectrophotometer. Transmission electron microscopy (TEM) was performed by LEO 912AB electron microscope. Ultrasonic bath (EUROSONIC® 4D ultrasound cleaner with a frequency of 50 kHz and an output power of 350 W) was used to disperse materials in solvents. Thermogravimetric analysis (TGA) was carried out using STA 1500 instrument at a heating rate of 10 °C min⁻¹ in air. The elemental analysis (CHN) was done by a conventional combustion method based on burning off the sample, and detecting the gases by a thermo conductivity detector (TCD). X-ray powder diffraction (XRD) data were collected on an XD-3A diffractometer using Cu K α radiation. X-ray photoelectron spectroscopy (XPS) was performed using a VG multilab 2000 spectrometer (ThermoVG scientific) in an ultrahigh vacuum. Ultraviolet–Visible (UV-Vis) spectra were obtained using a Shimadzu UV-2100 spectrophotometer. Scanning electron microscope (SEM) was performed on a Zeiss Supra 55 VP SEM instrument. The specific surface area was

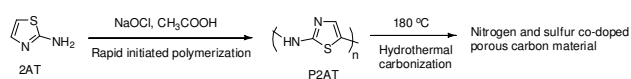
calculated using the Brunauer–Emmett–Teller (BET) equation using a PHS-1020(PHSCINA) device. Pore size distribution was determined by Barrett–Joyner–Halenda (BJH) method. The samples were degassed at 150 °C for 20 h before measurements. AA-680 Shimadzu (Kyoto, Japan) flame atomic absorption spectrometer (AAS) with a deuterium background corrector was used for determination of the metal. The conversions were obtained using a Varian 3900 GC.

2.3. Synthesis of poly(2-aminothiazole)

The special morphology of P2AT has been synthesized under rapid initiated conditions. In a typical synthesis, 25 ml aqueous solution of 2-aminothiazole (0.13 M) was mixed with 25 ml aqueous solution of acetic acid (0.13 M) under ultrasonic stirring for 2 min. Then 25 mL aqueous solution of sodium hypochlorite (0.065 M) as an oxidant was added into the above mixture quickly and immediately stirring or shaking to ensure sufficient mixing before polymerization begins. The solutions were cooled in a refrigerator at 10 °C for 10 min before the reactants were mixed. The polymerization reaction was carried out for 12 h at the specified temperature without any disturbance. Reaction mixture was neutralized by 0.01 M KOH solution. The resulting solid product was isolated by centrifugation and washed with MeCN (2 \times 30 mL) and hot water (2 \times 30 mL) to separate unreacted monomer and mineral salts, respectively. Finally, the product was dried under vacuum at room temperature for 24 h (Scheme 1).

2.4. Synthesis of N and S co-doped porous carbon structure derived from P2AT

The N and S co-doped porous carbon structure was synthesized with a combined hydrothermal and freeze-drying process. Typically, P2AT was firstly dispersed in water with ultrasonication reaching a concentration up to 3 mg mL⁻¹. A 5 mL aqueous dispersion of P2AT (3 mg mL⁻¹) was sonicated for 5 min, and then, the mixture was transferred to a teflon-lined autoclave and hydrothermally treated at 180 °C for 10 h. Finally, the resulting sample was freeze-dried to obtain the dual-doped porous carbon structure (Scheme 1).



Scheme 1 Synthesis of N and S co-doped porous carbon structure derived from P2AT.

2.5. Synthesis of gold nanoparticles immobilized on N and S co-doped porous carbon structure derived from P2AT

Aqueous solution of HAuCl₄·3H₂O (1 mg in 2.0 mL) and (N, S)-PCM (56 mg in 5.0 mL) were mixed and placed in an ultrasonic bath for 30 min to well disperse metal ions through the nitrogen and sulfur doped carbon structure. Then 4.8 mL of a 0.1 M NaBH₄ solution was added to mixture to reduce and form gold nanoparticles. After stirring for 4 h, it was filtered under vacuum, washed well with ethanol and water and dried under vacuum at 50 °C for 12 h.

2.6. General procedure for the catalytic reduction of nitrobenzenes

The reduction of 2-nitroaniline (2-NA) with NaBH_4 was carried out as a model reaction to examine the catalytic activity and reusability of the $\text{AuNPs}@(\text{N}, \text{S})\text{-PCM}$ catalyst. Amounts of 1.5 mL of deionized water, 500 μL of 2-NA aqueous solution (2 mM), and 100 μL of fresh NaBH_4 (0.2 M) were added into a flask in sequence, followed by addition of 40 μL of catalyst (1 mg mL^{-1}) to the mixture. The progress of the reaction was monitored by tracking the changes in the UV-vis absorption spectra of the mixture. After the reaction completion, the catalyst was removed and then reused in the next cycle. The catalytic reduction reactions of other nitrobenzenes were conducted under the same condition of 2-NA.

The catalytic reduction of 2-nitroaniline with H_2 was also investigated. For a typical hydrogenation procedure, 0.02 g $\text{AuNPs}@(\text{N}, \text{S})\text{-PCM}$, 1 mmol of 2-NA and 15 ml of deionized water were charged in the flask. The hydrogenation was taking place under magnetic stirring and an atmospheric hydrogen pressure at 30°C .

3. Results and discussion

3.1. Synthesis and recognition of the catalyst

At first, the polymerization of 2-aminothiazole was accomplished by the rapid mixing method using acetic acid as a dopant and sodium hypochlorite as an oxidant with the special ratios of 1:1 for monomer: dopant and 2:1 for monomer: oxidant. To confirm the successive synthesis of P2AT, FT-IR was employed, which is in good accordance with the literature²⁶ (See Fig. S1A). The morphology of the as-obtained poly(2-aminothiazole) was investigated by SEM as shown in Figure 1A-C.

As can be seen in the SEM image, a special plate structure with the height of approximately 8-10 μm consisting of nanoparticles was obtained. According to Brunauer-Emmett-Teller (BET) method, the surface area of P2AT was calculated to be $38.54 \text{ m}^2 \text{ g}^{-1}$.

Moreover, according to the obtained results from TGA (Fig. 2A), P2AT thermally degrades in four steps. 1.2% weight loss below 100°C is attributed to loss of moisture, adsorbed solvent or monomer. The major weight loss occurred on $200\text{--}600^\circ\text{C}$ is related to the conversion of P2AT to various subunits including NH_3 , HCN , CS_2 and carbene residue. DTA curve of P2AT is given in Fig. S2.

After the synthesis and characterization of P2AT, the hydrothermal carbonization following by freeze drying process were employed for synthesis of nitrogen and sulfur co-doped porous carbon structure. The hydrothermal carbonization reaction was carried out at mild temperature (180°C) and in pure water inside sealed autoclave and under self-generated pressure. It has been shown that hydrothermal carbonization leads to the more technical and structurally well-defined charring by a controlled chemical method which justifies its extensive application to produce various carbonaceous materials with attractive structures.

FT-IR spectrum of the as-obtained nitrogen and sulfur co-doped porous carbon material derived from P2AT was given in

Fig. S1C. The peaks at 1627 and 614 cm^{-1} attributed to the C=N and C-S stretching vibrations, respectively, are observed.

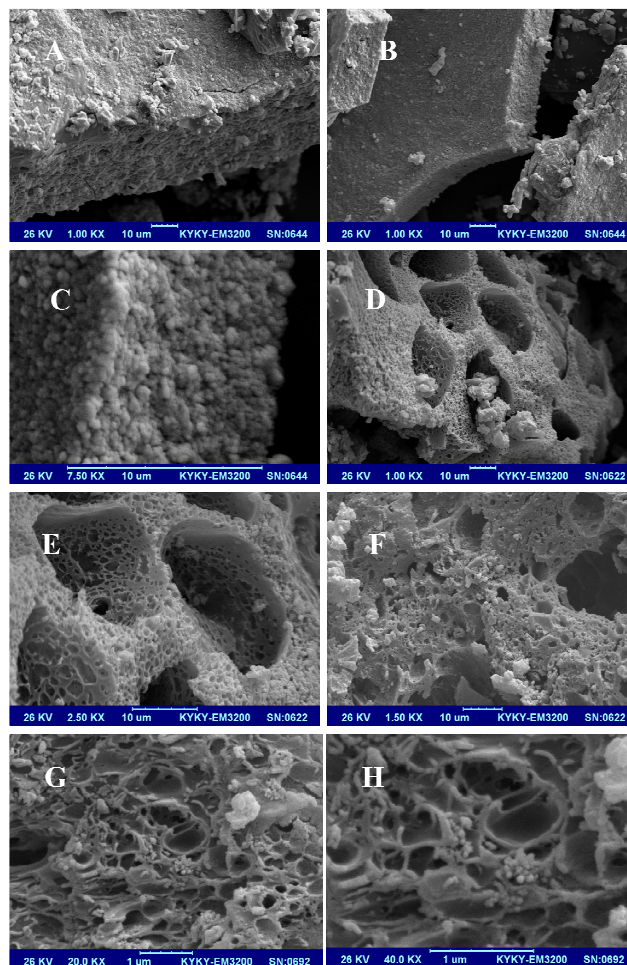


Fig. 1 SEM images of P2AT (A-C), (N, S)-PCM (D-F), and $\text{AuNPs}@(\text{N}, \text{S})\text{-PCM}$ (G, H).

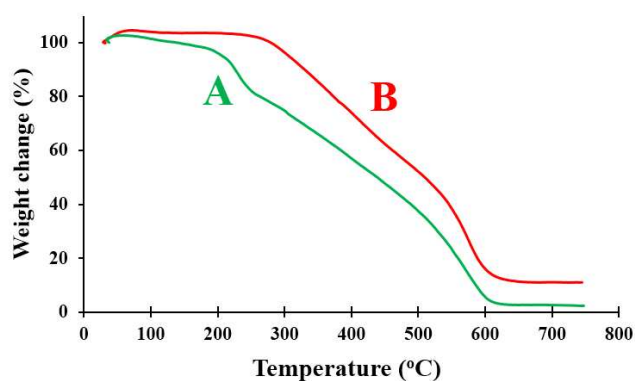


Fig. 2 TGA curves of P2AT (A) and (N, S)-PCM (B).

Morphological study of (N, S)-PCM was accomplished by SEM which is shown in Fig. 1 D-F. The pumice like morphology including pores inside the pores ranges from a several nanometers to micrometers can be observed in the SEM images of the synthesized material. One of the most important

factors for choosing a material as a support for catalytic application is its surface area. The surface area of (N, S)-PCM was determined by BET method to be $334.3 \text{ m}^2 \text{ g}^{-1}$. BET testing also showed a mesoporous and macroporous structure with the average pore sizes of 2.1 nm from analysis of the adsorption branch by the Barrett–Joyner–Halenda (BJH) method. To investigate the thermal stability of (N, S)-PCM, TGA analysis was performed which showed that the weight loss starts at 280°C (Fig. 2B).

In comparison with the XRD pattern of P2AT (Fig. 3A), the hydrothermal carbonization product represents a strong and wide peak at 2θ of 24.7° assigned to the hexagonal graphite (002) reflection ($2\theta = 26^\circ$).⁴⁰ The shift to the lower value is due to the presence of sulfur atoms, and can be directly associated to the much larger size of the sulfur atom than carbon or nitrogen.^{41,42} Since nitrogen was also doped which compresses the layers due to higher polarization interactions and so compensates the effect, the change in position of the (002) peak is lower compared to other sulfur doped reports.

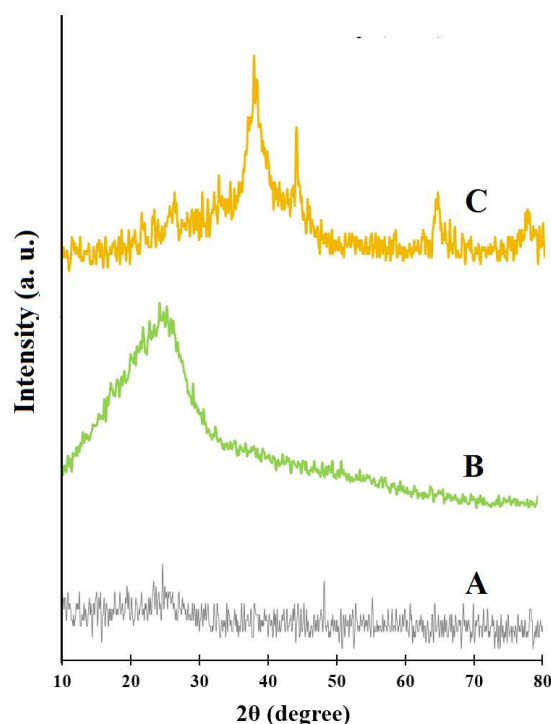


Fig. 3 XRD patterns of P2AT (A), (N, S)-PCM (B), and AuNPs@(N, S)-PCM (C).

XPS, as one of the most versatile techniques, was employed to investigate the composition of the as-synthesized material and the chemical states of the elements. The XPS spectrum of (N, S)-PCM has been presented in Fig. 4 which the peaks at 285, 532, 400, and 164 eV related to the C 1s, O 1s, N 1s, and S 2p are observed indicating the successful doping of S and N into the porous carbon structure by hydrothermal carbonization of P2AT. The chemical states of C, N and S in the (N, S)-PCM were further studied by high resolution XPS. The high-resolution spectrum of C1s in (N, S)-PCM can be divided into several

single peaks, corresponding to sp^2 -hybridized carbon atoms bound to neighboring carbon atoms or hydrogen (284.8 eV) and the peaks assigned to the electron-poor carbon bound to nitrogen or sulfur (286.0 eV),⁴³ and $-N-C(S)=N-$ (288.5eV),⁴⁴ further proving that N and S heteroatoms have been doped into the porous carbon structure. The bonding configurations of N and S atoms in the (N, S)-PCM were also investigated based on high-resolution N1s and S2p XPS spectra. The N1s peak in the XPS spectrum can be fitted into three peaks: pyridinic-like N (398.6), pyrrolic-like N (399.9) and graphitic-like N (401.2), which are typically observed in N-doped carbon materials.⁴⁵ Moreover, the high resolution S2p peak can be fitted with three different peaks at the binding energies of 164.0 ($S2p_{3/2}$), 164.9 eV ($S2p_{1/2}$), attributed to the sulfur binding in C–S bonds and conjugated $-C=S-$ bonds, and 168.8 eV related to the oxidized sulfur ($-SO_n-$).⁴⁶

The proposed precursor for N, S dual-doped carbon material was compared with recently reported precursors in terms of the procedure, heteroatom contents, and surface area, which the results have been summarized in Table 1. Elemental analysis (CHN) of (N, S)-PCM shows 55.77% C, 17.36% N, 2.54% H and 12.81% S. In addition, according to the XPS results, carbon, nitrogen, sulfur and oxygen contents are 57.93, 14.2, 4.45, and 23.42 at.%, which shows that the (N, S)-PCM displays a high number of heteroatom-doping, with N:C and S:C ratios of up to 1:4 and 1:13. Among several important reports, our precursor presents much higher amounts of heteroatom doping which makes it unique for various applications. Moreover, in the most cases, high temperatures and complicated processes are required to obtain the N, S co-doped carbon materials, while we use a simple hydrothermal treatment. Actually, employing P2AT as the precursor provides the advantages of a single step reaction with only one compound as a source of N and S under relatively mild conditions, high contents of the heteroatoms, high surface area, and gram-scale product. Therefore, due to the one-pot and straightforward synthesis, high surface area and also the presence of nitrogen and sulfur-dual doped in the as-prepared material, it seems that it can be an ideal choice to embed metal nanoparticles specially for catalytic applications. Furthermore, after the successful synthesis and characterization of (N, S)-PCM, gold nanoparticles were introduced to the support by the reduction of $\text{HAuCl}_4 \cdot 3\text{H}_2\text{O}$ using NaBH_4 .

To study the morphology of the (N, S)-PCM after the immobilization of AuNPs, SEM analysis was accomplished as shown in Fig. 1G and H. As can be seen, the porous structure of the carbon material was retained but its morphology was changed due to the loading of AuNPs on their surfaces.

Transmission electron microscope (TEM) analysis on AuNPs@(N, S)-PCM reveals the synthesis of ultra-small, monodisperse AuNPs with diameters between 1–4 nm on the (N, S)-PCM (Fig. 5). It was expected that due to the presence of both nitrogen and sulfur in the synthesized material, the support could stabilize Au nanoparticles with excellent dispersity.

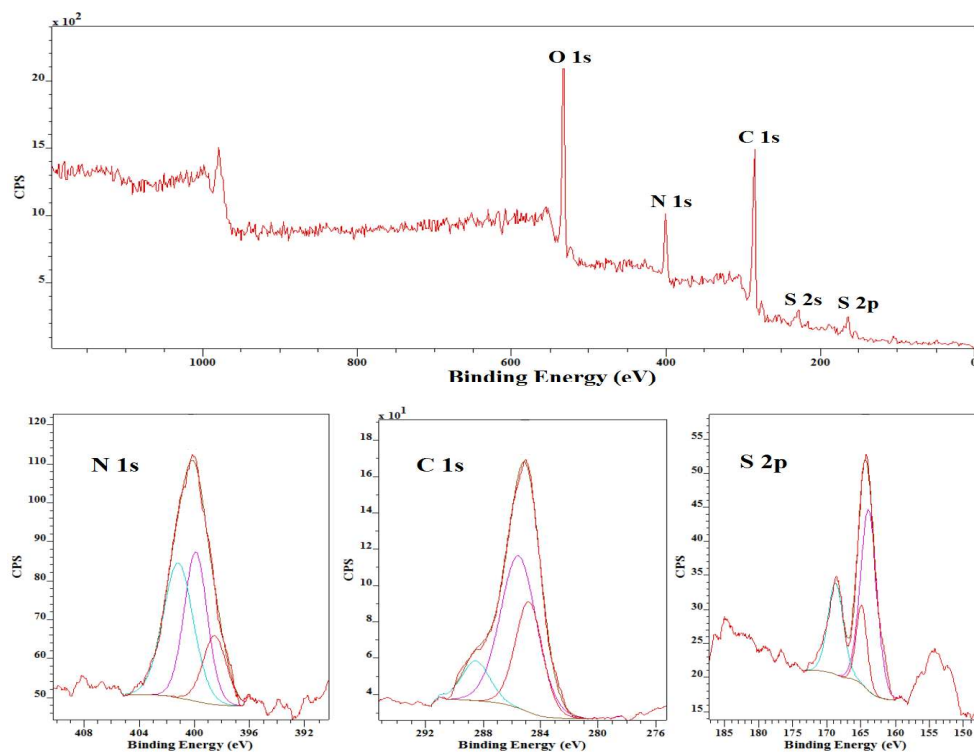


Fig. 4 XPS spectrum of AuNPs@(N, S)-PCM, and high resolution XPS spectra of S 2p, C 1s, and N 1s.

Table 1. Several reported precursors for N, S co-doped carbon materials.

Entry	Precursor for nitrogen and sulfur doping	Procedure	Amount of doping/Amount of	N- S-	Surface area m^2/g	Ref.
1	Cyanamide (N-doping), $FeSO_4/7H_2O$ (S-doping)	Carbonization at 1050 °C	0.9/0.6 (at.%)	-	-	47
2	Thiophene/acetoneitrile	Pyrolysis at 900 °C	7.6–8.3/0.7–1.6 (at.%)	150–240	48	
3	Cysteine	Pyrolysis at 900 °C	2.7/2.74 (wt.%)	180.5	43	
4	Thiourea and formaldehyde	Heating at 800 °C	8.5–17/3–8 (wt.%)	81–850	49	
5	Thiazolium salts: 3-methyl-thiazol-3-ium-dicyanamide and 3-(cyanomethyl)-thiazol-3-iumbromide	Carbonization at 1000 °C	5.19–6.17/2.17–3.84 (wt.%)	1174 and 1195	50	
6	S-(2-thienyl)-L-cysteine or 2-thienyl carboxaldehyde	Pyrolysis at 900 °C	4.3–5/0.74–1.0 (wt.%)	224.5 and 321	51	
7	Melamine (N-doping), benzyl disulfide (S-doping)	Heating at 900 °C	4.5/2.0 (at.%)	157–220	52	
8	Human hair (keratin containing cysteine)	Hydrothermal treatment at 180 °C, Heating at 600 °C	2.6–3.1/0.2–1.3 (at.%)	849–897	53	
9	SBA-15, sucrose and thiourea	Annealing at 1000 °C	6.53/2.88 (at.%)	394	45	
10	Citric acid as the carbon source, L-cysteine as nitrogen and sulfur source	Hydrothermal treatment, 200 °C	-	-	54	
11	Pyrrole and sulfuric acid	Carbonization at 650–950 °C	4.8–10/1.7–2.6 (at.%)	978–1021	55	
12	KIT-6 as the template and pyrrole as the precursor	Carbonization at 650–950 °C	10.0–4.6/0.94–0.75 (at.%)	1064, 693, and 880 depends on temperature	56	
13	Graphene oxide, thiourea	Annealing at 700 °C	~6.5/0.63 (at.%)	-	57	
14	Poly(2-aminothiazole)	Hydrothermal treatment, 180 °C	14.2/4.45 (at.%)	334.3	This work	

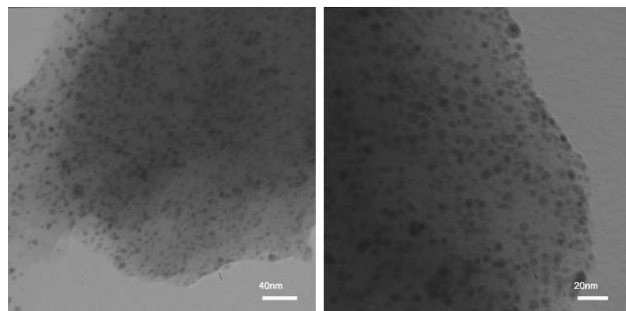


Fig. 5 TEM images of AuNPs@(N, S)-PCM.

We further characterized the AuNPs@(N, S)-PCM using XRD (Fig. 3C). (N, S)-PCM shows a broad diffraction peak for C(002) at $2\theta=24.7^\circ$ and is interpreted in terms of short-range order in stacked carbon sheets, but in AuNPs@(N, S)-PCM, the diffraction peak for C(002) is negligible indicating that significant face-to-face stacking is absent and suggesting that the carbon sheets were exfoliated due to the loading of AuNPs on their surfaces.⁵⁸ In addition, two strong bands are observed at $2\theta = 37.90^\circ$ and 44.05° , which correspond to the (111) and (200) crystallographic planes of AuNPs, and two additional peaks appear at $2\theta = 64.47^\circ$ and 77.50° related to the (220) and (311) crystallographic planes, respectively,⁵⁹ which are in good agreement with reference to fcc structure of metallic gold (JCPDS File No. 01-1174). The broadening of Bragg's peaks shows the formation of nanoparticles. According to the Scherrer equation based on the (111) peak line-width at half-maximum intensity, the average size of AuNPs was estimated to be 2.2 nm which is in good agreement with TEM results.

The Nitrogen adsorption isotherms of P2AT, (N, S)-PCM and AuNPs@(N, S)-PCM and pore-size distributions obtained from adsorption branch using the BJH method have been presented in Fig. S3. According to the BET measurements of AuNPs@(N, S)-PCM, the surface area of the catalyst with 2.0 nm pore sizes are estimated to be around $174.9 \text{ m}^2/\text{g}$, thus decreasing greatly with Au nanoparticle loading compared to $334.3 \text{ m}^2 \text{ g}^{-1}$ for (N, S)-PCM. This may be caused by a partial blockage of the (N, S)-PCM pores by AuNPs and/or a partial collapse of the mesoporous structure.

3.2. Catalytic activity

The catalytic activity of the as-synthesized gold nanoparticles immobilized on sulfur and nitrogen co-doped porous carbon was investigated by choosing the reduction reaction of 2-nitroaniline with NaBH_4 as a model reaction. This reaction, despite being thermodynamically favorable, does not occur spontaneously due to the presence of a kinetic barrier, but in the presence of metal nanoparticles as catalyst, the kinetic barrier was overcome through facilitating electron transfer from the donor BH_4^- to the acceptor 2-nitroaniline.⁶⁰ Since 2-Nitroaniline displays a typical absorbance peak at 410 nm which decreases as it is converted to 1,2-benzenediamine, the progress of the reaction could be easily monitored by UV-vis (Fig. S4). According to the result, 2-nitroaniline was completely reduced after 12 min.

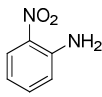
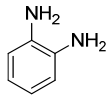
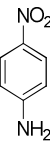
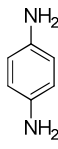
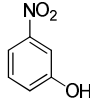
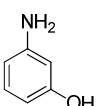
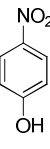
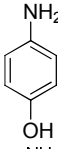
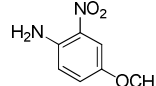
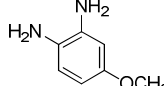
To show the role and performance of the support, and the possible usability of the support as a metal free catalyst, the catalytic reduction reaction of 2-nitroaniline was carried out using (N, S)-PCM under the same reaction conditions. According to the result, the reaction was completed after 56 min which indicated that the only support can be used as an efficient metal free catalyst for the reduction reactions. In 2013, Kong et al. reported the metal-free catalytic reduction of 4-nitrophenol to 4-aminophenol mediated by N-doped graphene. They suggested that the adsorption and activation of 4-nitrophenol ions only can be carried out by the carbon atoms next to the doped N atoms due to its weakened conjugation and higher positive charge density.⁶¹ In addition, the presence of S atoms in the (N, S)-PCM, may probably enhance the catalytic effect, due to its small band gap or a metallic form.⁶² Also, the π - π interactions of the aromatic group with the support prefers the close proximity of the reagents to the catalytic sites and establishing an efficient catalytic reduction.

To reveal the performance of the catalyst, several nitrobenzenes were subjected to the reduction reaction using NaBH_4 in the presence of AuNPs@(N, S)-PCM as the catalyst (Table 2, Fig. S5-8) which their complete conversion were reflected by the color change of the solution, from originally bright yellow to colorless. Since in the nitroarene reactions, the formation of diazo side products can significantly decrease the yields, the yields obtained by GC were also presented (Table 2). The presence of substituents such as OH, and NH_2 in ortho and para situations leads to the decreased activity towards reduction because of the electron-donating properties. The catalytic reduction of 2-nitroaniline with H_2 was also investigated which 1,2-benzenediamine was obtained with yield of 95% after 87 min.

The comparison of various AuNP catalysts of 2NA reduction with NaBH_4 as reducing agent is gathered in Table S1. The as prepared catalyst indicated good results compared to most of the reported catalysts in terms of mol% Au and time of reaction completion. Moreover, the synthesized support could be successfully employed as a metal free catalyst for catalytic reduction of 2-nitroaniline.

The catalyst stability and recyclability are important issues in the supported catalyst, so, we investigated the stability and recyclability of the as-synthesized catalyst by measuring the conversions up to six cycles after 4 min for reduction reaction of 2-nitroaniline as a model reaction (The reaction proceed was monitored by GC). The results are summarized in Fig. S9, proving the high stability and recyclability of the catalyst. Additionally, the leaching of the catalyst were investigated which interestingly, no leaching of active metal was occurred due to the high stability of Au nanoparticles.

Table 2 The catalytic reduction of nitrobenzenes with the AuNPs@(N, S)-PCM as the catalyst.^a

Entry	Compound	Product	Time (min)	Yield (%)
1			12	97
2			9	96
3			12	99
4			58	96
5			29	92

^a Reaction conditions: 1.5 mL of deionized water, 500 μL of nitrobenzenes aqueous solution (2 mM), and 100 μL of fresh NaBH_4 (0.2 M), 40 μL of AuNPs@(N, S)-PCM (1 mg mL^{-1}) at 25°C.

4. Conclusion

In this report, for the first time, the synthesis of P2AT with special morphology was presented by rapid mixing method. Subsequently, P2AT was used as a single source of nitrogen and sulfur to obtain N, S-co doped porous carbon by a simple hydrothermal carbonization reaction following by freeze drying. The SEM and BET results showed the high surface area and porosity of the synthesized material which makes it suitable as a support for catalytic applications. After the synthesis of (N, S)-PCM, very small and monodisperse gold nanoparticles were immobilized on it as proven by TEM and XRD analyses. The AuNPs@(N, S)-PCM exhibited high activity toward reduction reaction of nitrobenzenes.

Moreover, the applicability of the support as a metal free catalyst was evaluated for catalytic reduction of 2-nitroaniline showing very good results.

Acknowledgements

We are grateful to Shahid Beheshti University Research Council for partial financial support of this work.

Notes and references

- K. Gong, F. Du, Z. Xia, M. Durstock and L. Dai, *Science*, 2009, **323**, 760-764.
- S. Wang, D. Yu and L. Dai, *J. Am. Chem. Soc.*, 2011, **133**, 5182-5185.
- I. Kruusenberg, N. Alexeyeva, K. Tammeveski, J. Kozlova, L. Matisen, V. Sammelselg, J. Solla-Gullon and J. M. Feliu, *Carbon*, 2011, **49**, 4031-4039.
- Y. Li, W. Zhou, H. Wang, L. Xie, Y. Liang, F. Wei, J.-C. Idrobo, S. J. Pennycook and H. Dai, *Nat. Nanotechnol.*, 2012, **7**, 394-400.
- D. Yu, E. Nagelli, F. Du and L. Dai, *J. Phys. Chem. Lett.*, 2010, **1**, 2165-2173.
- P. Zhang, J. Lian and Q. Jiang, *Phys. Chem. Chem. Phys.*, 2012, **14**, 11715-11723.
- N. Alexeyeva, E. Shulga, V. Kisand, I. Kink and K. Tammeveski, *J. Electroanal. Chem.*, 2010, **648**, 169-175.
- G. P. Hao, G. Mondin, Z. Zheng, T. Biemelt, S. Klosz, R. Schubel, A. Eychmüller and S. Kaskel, *Angew. Chem. Int. Ed.*, 2014.
- N. Fechner, T.-P. Feller and M. Antonietti, *J. Mater. Chem. A*, 2013, **1**, 14097-14102.
- Y. Zheng, Y. Jiao, M. Jaroniec, Y. Jin and S. Z. Qiao, *Small*, 2012, **8**, 3550-3566.
- J. Kouvetakis, R. B. Kaner, M. L. Sattler and N. Bartlett, *J. Chem. Soc., Chem. Commun.*, 1986, 1758-1759.
- Q. Shi, F. Peng, S. Liao, H. Wang, H. Yu, Z. Liu, B. Zhang and D. Su, *J. Mater. Chem. A*, 2013, **1**, 14853-14857.
- D. Yu, Y. Xue and L. Dai, *J. Phys. Chem. Lett.*, 2012, **3**, 2863-2870.
- S. Wang, E. Iyyamperumal, A. Roy, Y. Xue, D. Yu and L. Dai, *Angew. Chem. Int. Ed.*, 2011, **50**, 11756-11760.
- J. P. Paraknowitsch and A. Thomas, *Energy Environ. Sci.*, 2013, **6**, 2839-2855.
- J. Liang, Y. Jiao, M. Jaroniec and S. Qiao, *Angew. Chem. Int. Ed.*, 2012, **51**, 11496-11500.
- W. Shen and W. Fan, *J. Mater. Chem. A*, 2013, **1**, 999-1013.
- J. P. Paraknowitsch and A. Thomas, *Macromol. Chem. Phys.*, 2012, **213**, 1132-1145.
- J. Yuan, A. G. Marquez, J. Reinacher, C. Giordano, J. Janek and M. Antonietti, *Polym. Chem.*, 2011, **2**, 1654-1657.
- J. P. Paraknowitsch, J. Zhang, D. Su, A. Thomas and M. Antonietti, *Adv. Mater.*, 2010, **22**, 87-92.
- M. R. Nabid, Y. Bide and Z. Habibi, *RSC Adv.*, 2015, **5**, 2258-2265.
- M. R. Nabid, Y. Bide and M. Abuali, *RSC Adv.*, 2014, **4**, 35844-35851.
- J. Cruz, E. Garcia-Ochoa and M. Castro, *J. Electrochem. Soc.*, 2003, **150**, B26-B35.
- A. Cukurovali, İ. Yılmaz, M. Ahmedzade and S. Kirbağ, *Heteroat. Chem.*, 2001, **12**, 665-670.
- X. Zhou, L. Shao, Z. Jin, J. B. Liu, H. Dai and J. X. Fang, *Heteroat. Chem.*, 2007, **18**, 55-59.
- M. Biyikoğlu and H. Çiftçi, *Polym. Bull.*, 2013, **70**, 2843-2856.
- M. Yıldırım and İ. Kaya, *Synth. Met.*, 2012, **162**, 436-443.
- J. Huang and R. B. Kaner, *Angew. Chem. Int. Ed.*, 2004, **43**, 5817-5821.
- S. J. T. Rezaei, Y. Bide and M. R. Nabid, *Synth. Met.*, 2011, **161**, 1414-1419.
- M. Reza Nabid, S. J. Tabatabaei Rezaei and S. Zahra Hosseini, *Mater. Lett.*, 2012, **84**, 128-131.
- Z. Li, C. Brouwer and C. He, *Chem. Rev.*, 2008, **108**, 3239-3265.
- A. Corma and H. Garcia, *Chem. Soc. Rev.*, 2008, **37**, 2096-2126.
- M. R. Nabid, Y. Bide and S. J. Tabatabaei Rezaei, *Appl. Catal., A*, 2011, **406**, 124-132.
- M. R. Nabid, Y. Bide and M. Niknezhad, *ChemCatChem*, 2014, **6**, 538-546.

- 35 M. R. Nabid and Y. Bide, *Appl. Catal., A*, 2014, **469**, 183-190.
- 36 M. R. Nabid, Y. Bide, E. Aghaghafari and S. Rezaei, *Catal. Lett.*, 2014, **144**, 355-363.
- 37 M. R. Nabid, Y. Bide, N. Ghalavand and M. Niknezhad, *Appl. Organomet. Chem.*, 2014, **28**, 389-395.
- 38 S. S. Muir and X. Yao, *Int. J. Hydrogen Energy*, 2011, **36**, 5983-5997.
- 39 O. Ozay, E. Inger, N. Aktas and N. Sahiner, *Int. J. Hydrogen Energy*, 2011, **36**, 8209-8216.
- 40 Z. Li, C. Lu, Z. Xia, Y. Zhou and Z. Luo, *Carbon*, 2007, **45**, 1686-1695.
- 41 S. Glenis, A. Nelson and M. Labes, *J. Appl. Phys.*, 1999, **86**, 4464-4466.
- 42 Y. Wu, S. Fang, Y. Jiang and R. Holze, *J. Power Sources*, 2002, **108**, 245-249.
- 43 C. H. Choi, S. H. Park and S. I. Woo, *Green Chem.*, 2011, **13**, 406-412.
- 44 N. Baccile, M. Antonietti and M.-M. Titirici, *ChemSusChem*, 2010, **3**, 246-253.
- 45 Z. Liu, H. Nie, Z. Yang, J. Zhang, Z. Jin, Y. Lu, Z. Xiao and S. Huang, *Nanoscale*, 2013, **5**, 3283-3288.
- 46 S. Yang, L. Zhi, K. Tang, X. Feng, J. Maier and K. Müllen, *Adv. Funct. Mater.*, 2012, **22**, 3634-3640.
- 47 H. T. Chung, C. M. Johnston, K. Artyushkova, M. Ferrandon, D. J. Myers and P. Zelenay, *Electrochem. Commun.*, 2010, **12**, 1792-1795.
- 48 E. J. Biddinger, D. S. Knapke, D. von Deak and U. S. Ozkan, *Appl. Catal., B*, 2010, **96**, 72-82.
- 49 T. Tsubota, K. Takenaka, N. Murakami and T. Ohno, *J. Power Sources*, 2011, **196**, 10455-10460.
- 50 J. P. Paraknowitsch, B. Wienert, Y. Zhang and A. Thomas, *Chem. Eur. J.*, 2012, **18**, 15416-15423.
- 51 S.-A. Wohlgemuth, R. J. White, M.-G. Willinger, M.-M. Titirici and M. Antonietti, *Green Chem.*, 2012, **14**, 1515-1523.
- 52 J. Liang, Y. Jiao, M. Jaroniec and S. Z. Qiao, *Angew. Chem. Int. Ed.*, 2012, **51**, 11496-11500.
- 53 W. Si, J. Zhou, S. Zhang, S. Li, W. Xing and S. Zhuo, *Electrochim. Acta*, 2013, **107**, 397-405.
- 54 Y. Dong, H. Pang, H. B. Yang, C. Guo, J. Shao, Y. Chi, C. M. Li and T. Yu, *Angew. Chem. Int. Ed.*, 2013, **52**, 7800-7804.
- 55 D. Zhang, Y. Hao, L. Zheng, Y. Ma, H. Feng and H. Luo, *J. Mater. Chem. A*, 2013, **1**, 7584-7591.
- 56 D. Zhang, L. Zheng, Y. Ma, L. Lei, Q. Li, Y. Li, H. Luo, H. Feng and Y. Hao, *ACS appl. Mater. Inter.*, 2014, **6**, 2657-2665.
- 57 X. Wang, J. Wang, D. Wang, S. Dou, Z. Ma, J. Wu, L. Tao, A. Shen, C. Ouyang and Q. Liu, *Chem. Commun.*, 2014, **50**, 4839-4842.
- 58 Y. Si and E. T. Samulski, *Chem. Mater.*, 2008, **20**, 6792-6797.
- 59 M. J. Rak, N. K. Saadé, T. Friščić and A. Moores, *Green Chem.*, 2014, **16**, 86-89.
- 60 J. Huang, L. Zhang, B. Chen, N. Ji, F. Chen, Y. Zhang and Z. Zhang, *Nanoscale*, 2010, **2**, 2733-2738.
- 61 X.-k. Kong, Z.-y. Sun, M. Chen and Q.-w. Chen, *Energy Environ. Sci.*, 2013, **6**, 3260-3266.
- 62 P. A. Denis, R. Faccio and A. W. Mombru, *ChemPhysChem*, 2009, **10**, 715-722.